Available online at www.sciencedirect.com
SCIENCE DIRECT®
Tetrahedron
Tetrahedron 60 (2004) 3473–3485

1,3-Dipolar cycloaddition of stabilised and non-stabilised azomethine ylides derived from uracil polyoxin C (UPoC): access to nikkomycin analogues

H. Ali Dondas,[a,b] Colin W. G. Fishwick,[a] Ronald Grigg[a,*] and Colin Kilner[a]

[a]*Molecular Innovation, Diversity and Automated Synthesis (MIDAS) Centre, Department of Chemistry, The University of Leeds, Leeds LS2 9JT, UK*
[b]*Department of Chemistry, Faculty of Pharmacy, Mersin University, Mersin, Turkey*

Received 26 September 2003; revised 21 January 2004; accepted 12 February 2004

Abstract—Cascade thermal and decarboxylative cycloaddition reactions of uracil polyoxin C (UPoC) with mono- and di-carbonyl compounds in the presence of a dipolarophile leads, via stabilised and non-stabilised azomethine ylides respectively, to a series of polyoxin cycloadducts related to Nikkomycin B in good to excellent yields and high diastereoselectivity.

1. Introduction

The nikkomycins[1] and neopolyoxins[2] are a group of nucleoside di- and tri-peptide antibiotics produced by *Streptomyces tandea* and *S. cocaoi ssp. asoensis*. Representative examples of these intriguing natural products include nikkomycin B (**1**), nikkomycin J (**2**) and nikkomycin Bx (**3**). These compounds are potent chitin synthetase inhibitors and they exhibit fungicidal, insecticidal and acaricidal activities.[1,2] The inhibition of *botrytis cinerea*, *pyricularia oryzae*, and *candida albicans* by the neopolyoxins is particularly noteworthy.[2]

Uracil polyoxin C (UPoC)[3] (**4**) is the carboxy terminal nucleoside amino acid common to many members of the polyoxin and nikkomycin family and is a versatile relay intermediate for the synthesis of analogues.[2,4] The polyoxins (**5**)[5] exhibit marked and selective activity against phytopathogenic fungi whilst being non-toxic to bacteria, plants, or animals.[6] Their effectiveness against *candida albicans* is particularly important since this organism causes major disease problems for AIDS patients.[7] As a consequence of these biological effects derivatives of these compounds are attractive targets for synthesis.

The decarboxylative route to azomethine ylides via imines of α-amino acids when coupled to a subsequent cycloaddition[8–11] has provided access to bicyclic pyrrolidines,[8] biomimetic examples of the mode of action of pyridoxal and pyruvate based enzyme decarboxylases,[9] a new route to spirocyclic and bridged-ring compounds,[10,11] and medium rings via ring expansion of cyclic secondary α-amino acids.[12] This versatile methodology has now been applied to the synthesis of new analogues of UPoC.

2. Decarboxylative cycloaddition reactions

Cascade thermal reactions of uracil polyoxin C (UPoC) with mono- and di-carbonyl compounds in the presence of *N*-methylmaleimide (NMM) and *N*-phenyl maleimide (NPM) leads, via an intermediate azomethine ylide, to a series of polyoxin cycloadducts in excellent yield.

The reactions were performed in DMF using 2 mol equiv. of carbonyl compound and 1 mol equiv. of *N*-methyl maleimide or *N*-phenyl maleimide. Thus UPoC (**4**) reacted with methyl pyruvate and NMM or NPM (DMF, 70 °C, 26 h) to afford 9:1 and 12:1 mixtures of cycloadducts (**6a**, **7a**) and (**6b**, **7b**) respectively in 94 and 96% yield. The relative stereochemistry of the pyrrolidinyl substituents of the major chiral *endo*-isomers (**6a**) and (**6b**) were determined from NOE data and 2D-COSY studies. In the case of (**6a**) irradiation of 3-H effected enhancement of the signals for 1-Me (6%) and 3a-H (7.95%) whilst irradiation of 3a-H effected enhancement of the signals for 3-H (5.65%) and 6a-H (4.4%). Irradiation of 1-Me effected enhancement of

Keywords: Uracil polyoxin C; Nikkomycin; Azomethine ylide; 1,3-Dipolar cycloaddition; Chitin synthetase inhibitors; Decarboxylative cycloaddition; Semi-empirical; Calculations.
* Corresponding author. Tel.: +44-1133436501; fax: +44-1133436530; e-mail address: R.Grigg@chemistry.leeds.ac.uk

0040–4020/$ - see front matter © 2004 Elsevier Ltd. All rights reserved.
doi:10.1016/j.tet.2004.02.028

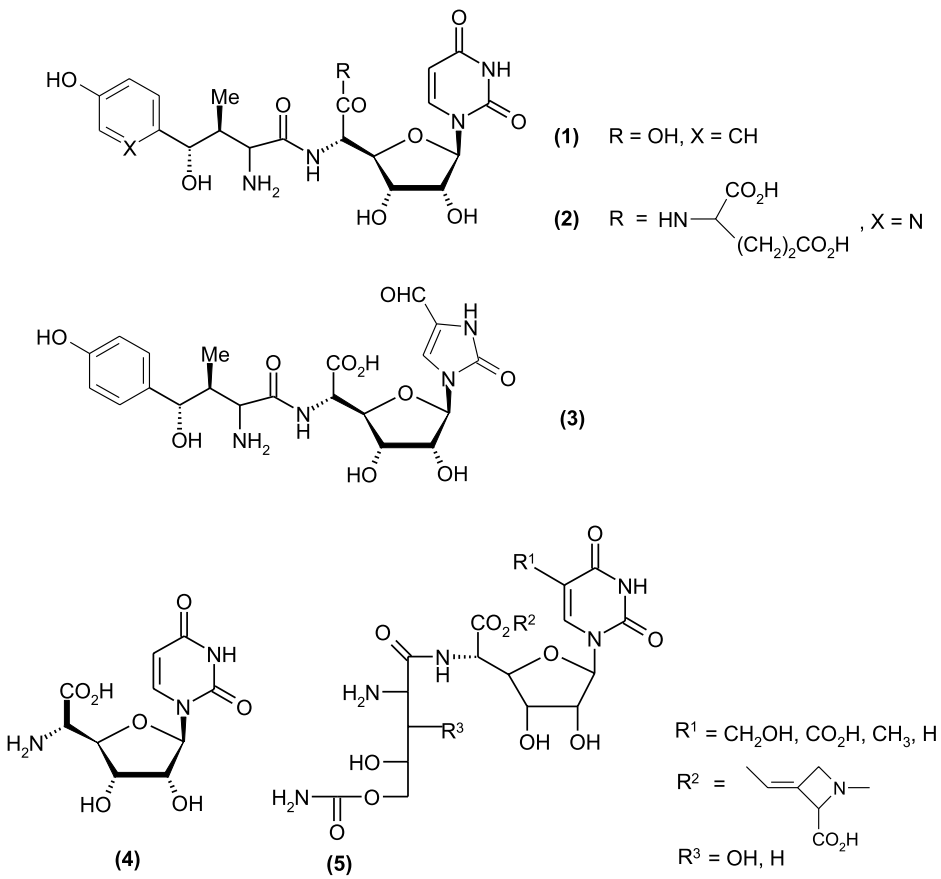

the signals for 6a-H (4.6%) and 3-H (2.25%). Irradiation of 3-H effected enhancement of coincident signals for 2′-H, 3′-H and 4′-H (11.3%) and irradiation of 3a-H effected enhancement of the signals for 2′-H, 3′-H and 4′-H (4.3%). There are two possible diastereoisomeric cycloadducts (**6a**) and (**7a**), arising from *endo*-cycloaddition to either diastereotopic face of the azomethine ylide *syn* 1 (**8**),[8,11] and these are indistinguishable from these data. However, the absolute stereochemistry of (**6b**) was determined by an X-ray crystal structure (Fig. 1).

Figure 1 unequivocally establishes the absolute stereochemistry of the new stereocentres created in the cycloaddition as 1*S*,3*S*,3a*S* and 6a*R*. Hence the cycloaddition proceeds via *endo* addition to the 1 (si), 3 (re)- face of *syn* 1 (**8**). The minor isomers could not be isolated in a pure form. The stereochemical preference for the formation of dipole *syn* 1 (**8**) is discussed in detail later.

UPoC (**4**) reacted with benzaldehyde and NMM under the same conditions over 24 h to yield a 3:1 mixture of cycloadducts (**6c**) and (**7c**) in 78% combined yield. The minor isomer could not be isolated in a pure form. The stereochemistry of the major *endo*-product (**6c**) was established from NOE data and 2D-COSY studies. Thus irradiation of 3-H effected enhancement of coincident signals for 3a-H+6a-H (4.2%) and irradiation of 1-H effected enhancement of the signals for 3a-H+6a-H (11.8%) and 3-H (4.9%). Irradiation of 3-H effected enhancement of the signals for 3′-H (8.2%) and irradiation of 1-H effected enhancement of the signals for 2′-H (9.7%). Irradiation of 2′-H effected enhancement of the signals for 1-H (9.7%) and 3a-H+6a-H (4.35%).

Reaction of (**4**) with 2-pyridine carboxaldehyde and NMM occurred over 22 h in DMF at 65 °C to afford a 4:3 mixture of cycloadducts (**6d**) and (**7d**) (52%). The isomeric mixture could not be separated and analysis of the ^{1}H NMR spectrum of the mixture was difficult due to overlapping signals. Hence the relative stereochemistry of the major isomer was not firmly established but the protons were assigned based on 2D-COSY studies and by analogy with related systems.

The product from the reaction (DMF, 80 °C, 22 h) of UPoC (**4**), *N*-phenylsulphonyl indolyl-3-aldehyde and NMM consisted of a 1:1 mixture of cycloadducts (**6e**) and (**7e**) in 74% yield. The relative stereochemistry of the pyrrolidinyl substituents of (**6e**) was established from NOE data and 2D-COSY studies. Thus irradiation of 3a-H effected enhancement of the signals for 6a-H (5.5%) and 3-H (3.5%) whilst irradiation of 1-H effected enhancement of the signals for 6a-H (6%).

Isatin, UPoC (**4**) and NMM react under similar conditions (DMF, 90 °C, 30 h) affording a 2:1 mixture of cycloadducts (**6f**) and (**7f**) in 82% combined yield. The second most abundant isomer could not be isolated in a pure form. The *cis*-3,3a-stereochemistry of the pyrrolidine ring of the major isomer (**6f**) was determined from NOE data [irradiation of 3a-H effected enhancement of the signals for 3-H (15%)]

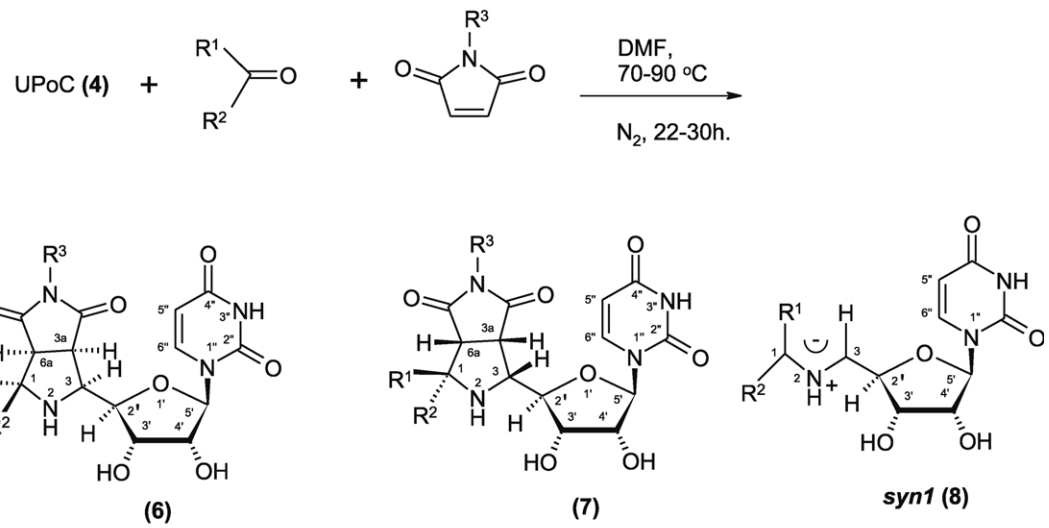

a R^1 = Me R^2 = CO_2Me R^3 = Me
b R^1 = Me R^2 = CO_2Me R^3 = Ph
c R^1 = H R^2 = Ph R^3 = Me
d R^1 = H R^2 =  R^3 = Me
e R^1 = H R^2 = 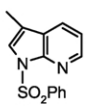 R^3 = Me
f R^1, R^2 =  R^3 = Me

a R^1 = Me R^2 = CO_2Me R^3 = Me
b R^1 = Me R^2 = CO_2Me R^3 = Ph
c R^1 = H R^2 = Ph R^3 = Me
d R^1 = H R^2 =  R^3 = Me
e R^1 = H R^2 = 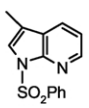 R^3 = Me
f R^2, R^1 =  R^3 = Me

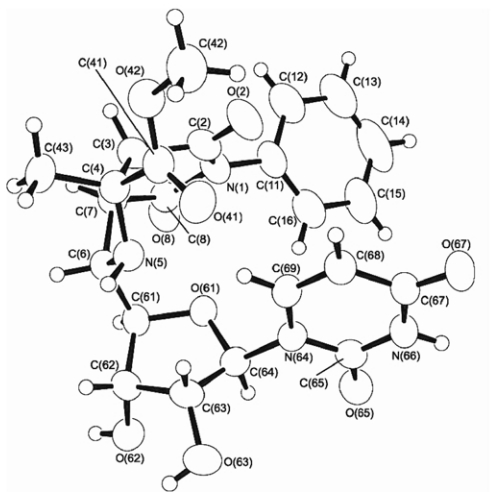

Figure 1. X-ray crystal structure of (**6b**).

whilst the stereochemistry at C-1 is assigned on the basis of previous studies.[13]

3. Cascade imine formation-prototropy-cycloaddition

UPoC methyl ester hydrochloride (**9**),[14] benzaldehyde and NMM were reacted (pyridine, $MgSO_4$, 100 °C, 28 h) to give a single cycloadduct (**11**) in 32% yield via azomethine ylide *syn* 1 (**10**) (Scheme 1). The relative stereochemistry of the pyrrolidinyl substituents of (**11**) was established from NOE data and 2D-COSY studies. Thus irradiation of 1-H effected enhancement of the signals for 6a-H (10.6%) whilst irradiation of 6a-H effected enhancement of the signals for

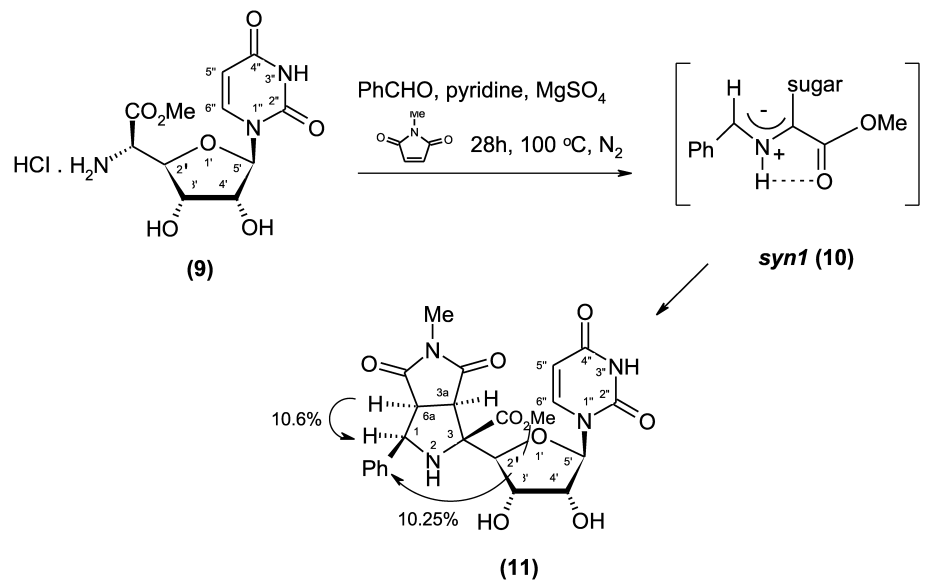

Scheme 1. Stereoselective in situ formation and cycloaddition of dipole (**10**).

1-H (10.15%) and 3a-H (8.45%). Irradiation of 3a-H effected enhancement of the signals for 6a-H (12.3%) and irradiation of CO_2Me effected enhancement of the signals for ArH (10.25%). Again there are two possible *endo*-diastereoisomeric cycloadducts corresponding to *endo*-cycloaddition to the two diastereotopic faces of dipole *syn* 1 (**10**). We have rationalised the stereocontrol in these cycloadditions using semi-empirical calculations as described below (Scheme 2).

4. Rationalisation of stereocontrol using semi-empirical calculations

The stereoselectivity observed in the cycloadditions of both dipoles (**8**) and (**10**) is remarkable, especially in light of the fact that each dipole can adopt four possible geometries (denoted *syn* 1, *anti* 1, *syn* 2, and *anti* 2 respectively, Scheme 2). Additionally, each of these four geometrical isomers can undergo cycloaddition from the

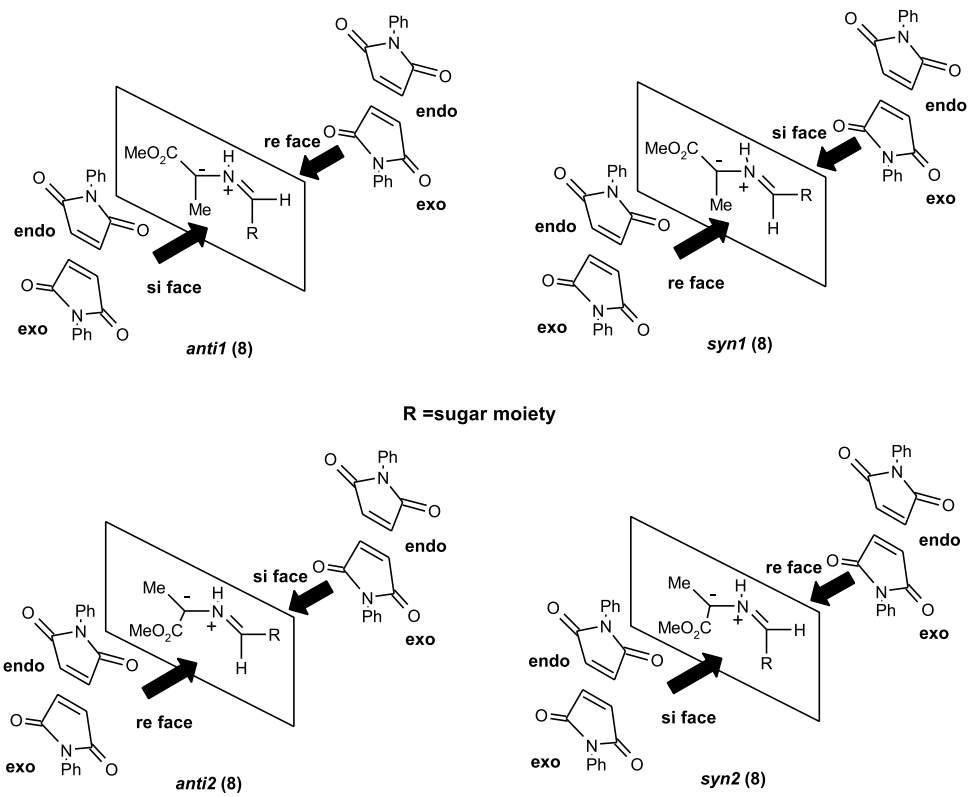

Scheme 2. Possible cycloaddition modes for *syn* 1, *syn* 2, *anti* 1, and *anti* 2 geometries of dipole (**8**).

Table 1. Calculated heats of formation, for 1,3-dipoles (**8**) and their cycloaddition transition states to NPM

Dipoles (**8**)/H_f[a]	H_f[a] and imaginary vibrational frequencies[b] ν_i of transition states from dipoles (**8**)							
	endo				*exo*			
	re		*si*		*re*		*si*	
syn 1, −253.47	−234.33	(−467.40)	−239.04	(−467.40)	−236.83	(−426.66)	−236.56	(−448.91)
anti 1, −231.73	−230.80	(−447.20)	−223.67	(−425.25)	−224.54	(−513.90)	−223.67	(−498.38)
syn 2, −247.65	−219.67	(−332.81)	−230.72	(−348.11)	−224.52	(−455.11)	−228.04	(−405.29)
anti 2, −253.52	−234.47	(−405.29)	−237.31	(−408.59)	−239.84	(−426.35)	−239.09	(−445.19)

[a] Heats of formation in kcal mol^{-1}, obtained using AM1 Hamiltonian after full geometry optimisation and corrected for solvation.[15]
[b] All transition structures were characterized by observing them to have a single negative vibrational frequency corresponding to the reaction coordinate following a normal mode analysis (figures in brackets in cm^{-1}).

Table 2. Calculated activation energies, E_a, for cycloaddition of dipoles (**8**) to NPM

Entry	Dipole (**8**)	Cycloaddition activation energies, E_a[a]			
		endo		*exo*	
		re	*si*	*re*	*si*
1	*syn* 1	19.56	14.85	17.06	17.33
2	*anti* 1	20.56	16.59	26.82	27.69
3	*syn* 2	28.40	17.34	23.55	20.03
4	*anti* 2	19.47	16.63	14.10	14.85

[a] Energies in kcal mol^{-1}. This energy is the difference between the sum of the heats of formation of dipole+NPM (H_f=−0.42 kcal mol^{-1}) and the heat of formation of the corresponding transition state.

two non-equivalent dipole faces (termed *re* and *si* respectively, where this refers to the prochirality at the carbon of the dipole attached to the sugar moiety, Scheme 2) and in both *endo* and *exo* modes (Scheme 2). We have used semi-empirical calculations to probe the factors that may give rise to the high diastereocontrol within these cycloadditions.

4.1. (a) Decarboxylative generation and subsequent cycloadditions of dipole (8)

We chose to investigate the cycloadditions of dipole **8**, (R^1=Me, R^2=CO_2Me) with *N*-phenyl maleimide (NPM), which had been observed to yield mainly one diastereoisomeric cycloadduct (**6b**) for which the stereochemistry had been unambiguously assigned using X-ray crystallography. The heats of formation of all the four geometric

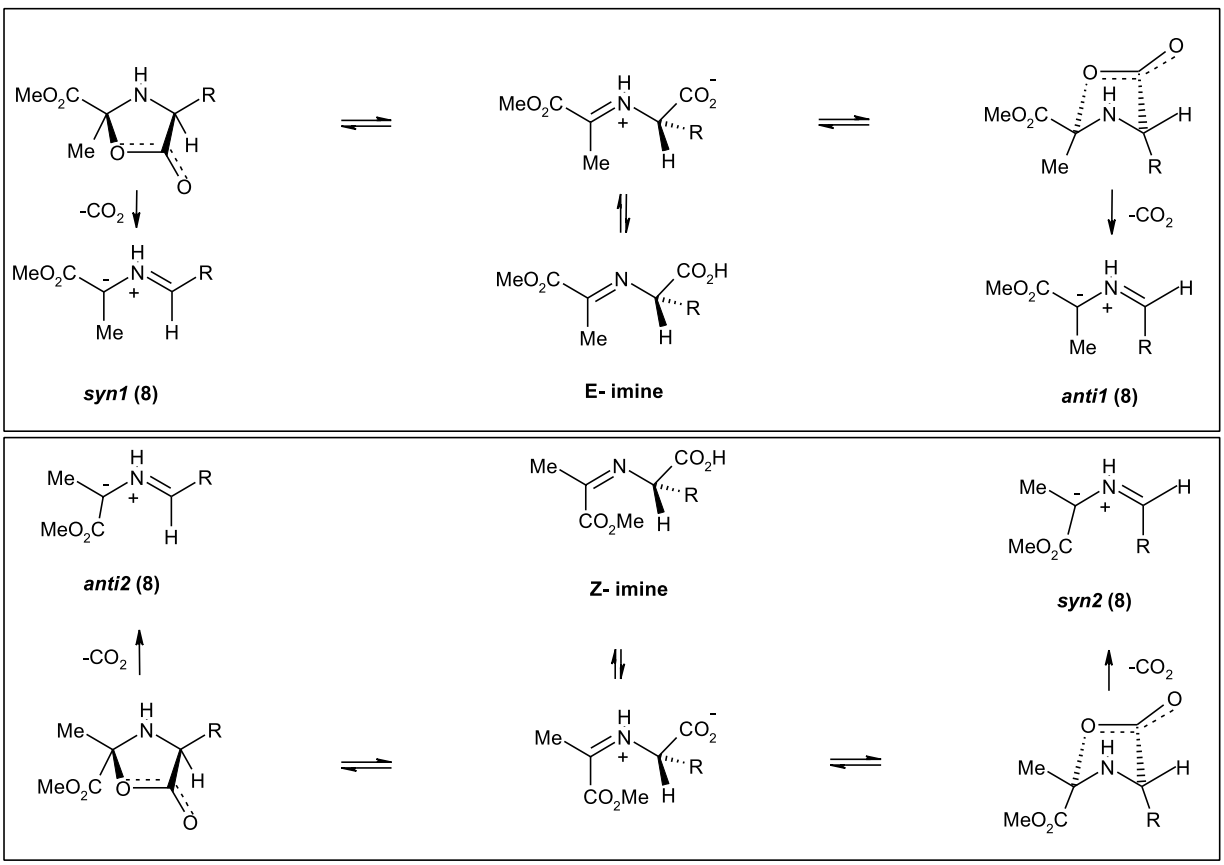

Scheme 3. Formation of 1,3-dipoles (**8**) from decarboxylation of imines.

Table 3. Calculated heats of formation for 1,3-dipoles (**8**) and their cycloaddition transition states to NPM

Entry	Reaction	H_f(TS)[a]	ν_i[b]	E_a[c]
1	*E*→*anti* 1 (**8**)	−324.72	−497.59	31.52
2	*E*→*syn* 1 (**8**)	−340.02	−497.59	16.22
3	*Z*→*syn* 2 (**8**)	−340.96	−497.59	26.71
4	*Z*→*anti* 2 (**8**)	−313.35	−497.59	53.32

[a] Heats of formation in kcal mol^{-1}, obtained using AM1 Hamiltonian after full geometry optimisation and corrected for solvation.[15]
[b] All transition structures were characterized by observing them to have a single negative vibrational frequency corresponding to the reaction coordinate following a normal mode analysis (figures in brackets and expressed in cm^{-1}).
[c] Energies in kcal mol^{-1}. This energy is the difference between the heat of formation of the transition state and that calculated for the corresponding imine (*E*-imine, H_f=−356.24 kcal mol^{-1}, *Z*-imine, H_f=−367.67 - kcal mol^{-1}).

forms of dipole (**8**) together with the 16 possible transition states (Scheme 2) for cycloaddition of (**8**) to *N*-phenyl maleimide, and the corresponding activation energies are shown in Tables 1 and 2.

Additionally, in order to establish a broad picture of the energetics involved in the whole reaction sequence, the generation of dipoles (**8**) via decarboxylative condensation of (**4**) with methyl pyruvate was investigated using semi-empirical calculations (Scheme 3). Each of the two possible imines resulting from the initial condensation can give rise to two particular dipoles respectively via decarboxylation (Scheme 3). The calculated heats of formation of each of the four decarboxylative transition states (H_f(TS)), together with the corresponding activation energies (E_a) are given in Table 3. Clearly these data indicate a strong preference for the reaction to proceed via decarboxylation of the E-imine to yield the *syn* 1 geometrical isomer of dipole (**8**), (Table 3, entry 2). Inspection of this transition structure reveals the existence of an intramolecular H-bond (length=2.14 Å) between the dipole NH and the C-2 carbonyl present on the uracil ring. (Fig. 2).

This transition structure also contains an H-bond (length=2.12 Å) between the C=O within the departing CO_2 molecule and the 3′-OH of the sugar (Fig. 2).

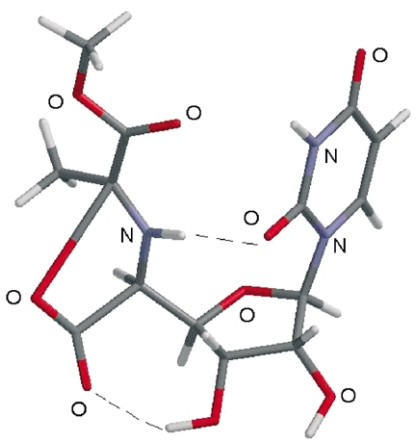

Figure 2. Calculated transition structure leading to dipole: syn 1 (8) showing H-bonding (dashed lines).

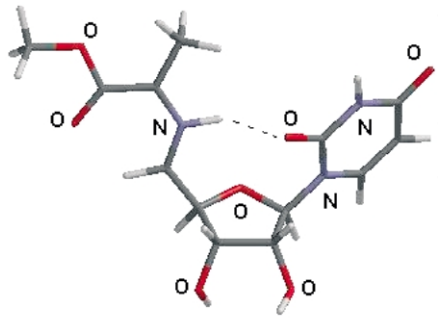

Figure 3. Calculated structure of *anti* 2 (**8**).

It would appear that this hydrogen bonding is important in stabilising this particular arrangement and promoting the formation of the *syn* 1 dipole. This intramolecular H-bonding feature involving the dipole N–H and uracil C=O is also apparent in the calculated structures of the *syn* 1- and *anti* 2-dipoles and here also appears to make important contributions in stabilising these dipole geometries (Figs. 3 and 4). The ubiquitous role of hydrogen bonding in structure and mechanism is well known[16] and these theoretical insights suggest novel ways of controlling dipole stereochemistry by distal functionality.

Another interesting feature of the transition structures from the decarboxylations is the very long C–O bond linking the departing CO_2 fragment to the dipole (see for example, Fig. 2). This implies that these decarboxylations are highly asynchronous and may be tend towards being more accurately described as involving CO_2 loss from an intermediate zwitterionic imminium carboxylate rather than from concerted decarboxylation from an intermediate oxazolidinone. As these calculations were performed in a simulated DMF solvent,[16] this asynchronicity would be expected to be maximised, and it would be interesting to investigate the effect of solvent polarity on the predicted mechanism of decarboxylation. In our previous studies on the stereochemistry[8] and mechanism[11] of related processes we had favoured the concerted route via the oxazolidinone.

The energetically favoured *E*→*syn* 1 (**8**) transition state restricts the reaction outcome to formation of an adduct derived from the *syn* 1-dipole (Table 2, entry 1). Here, the energetics clearly favour formation of the *endo* adduct

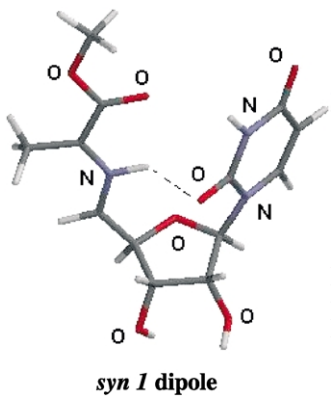

Figure 4. Calculated structure of dipole *syn* 1 (**8**).

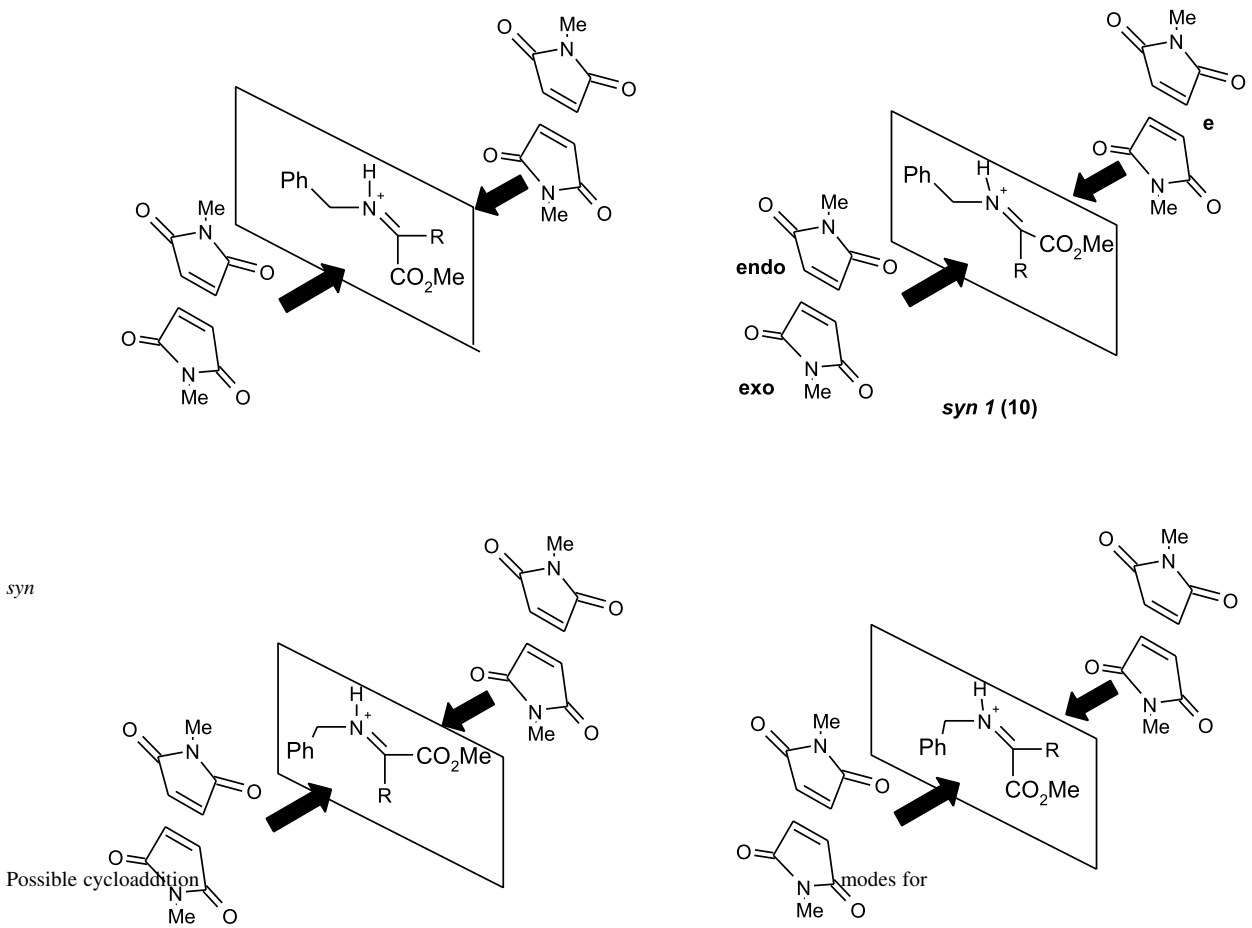

Scheme 4.

resulting from addition to the *si* face of the dipole to yield adduct (**6b**) in complete agreement with our experimental observations. This diastereoselectivity appears to be a direct consequence of the uracil-derived intramolecular H-bonding which acts to lock the conformation of the dipole and directs the attack of the dipolarophile from the least-hindered face of the dipole.

4.2. (b) 1,2-Prototropic generation and subsequent cycloadditions of dipole (10)

Similar geometrical outcomes to those for the cycloadditions of dipole (**8**) can be applied to the reaction of dipole (**10**) with NMM (Scheme 4).

The calculated heats of formation of the transition states and the corresponding activation energies for these various cycloaddition modes are given in Tables 4 and 5.

Unlike the case for the generation of dipoles (**8**) via irreversible decarboxylation, the generation of dipoles (**10**) presumably involves a reversible formal 1,2-prototropic shift in the initially formed imines following the condensation reaction. In terms of thermodynamic stability, this means that *syn* 1 dipole (**10**) will dominate this equilibrium as it is between 4.5 and 12 kcal mol^{-1} lower in energy than the alternative dipole geometries (Table 4, column 1). It is interesting that in the case of dipole (**10**), although the intramolecular H-bonding involving the uracil ring and the

and of transition states imaginary vibrational frequencies

Heats , of formation in kcal mol obtained using
All transition structures were characterized by observing them to have a single negative vibrational frequency corresponding to the reaction coordinate following a normal mode an

Table 5. Calculated activation energies, E_a, for cycloaddition of dipoles (**10**) to NMM

Entry	Dipole (**10**)	Cycloaddition activation energies, E_a[a]			
		endo		*exo*	
		re	*si*	*re*	*si*
1	*syn* 1	20.59	19.62	38.95	25.85
2	*anti* 1	21.53	23.34	19.95	16.16
3	*syn* 2	22.54	28.12	26.23	30.54
4	*anti* 2	22.45	106.38	30.39	26.06

[a] Energies in kcal mol^{-1}. This energy is the difference between the sum of the heats of formation of dipole+NMM (H_f=−11.06 kcal mol^{-1}) and the heat of formation of the corresponding transition state.

dipole N–H is present in the *anti* 1 and *syn* 2 geometries, these are not the most stable forms and both are higher in energy than the *syn* 1 form in which this H-bonding is absent. It is noted however that the *syn* 1 dipole has a considerably greater calculated electronic dipole moment (5.95 D in a simulated solvent environment) compared to that of either the *anti* 1 (2.44 D) or the *syn* 2 (2.02 D) dipoles and so presumably derives considerable stabilisation from the fact that the calculations were performed where solvation from a polar solvent is simulated.[15]

Within the possible transition structures resulting from cycloaddition of the *syn* 1 dipole, those due to an *endo* approach of the dipolarophile are clearly favoured over the *exo*-derived systems (entry 1, Table 5). The predicted balance between either *si* or *re* addition is essentially even however, with *si* addition only very slightly favoured over *re*. In fact, as described above, this reaction gives a moderate yield of adduct (**11**) whose stereochemistry corresponds to the predicted *syn* 1-*endo*-*si* cycloaddition mode. Based on our calculations, we would expect some of the alternative *syn* 1-*endo*-*re* adduct to have also been obtained, and although no other cycloadducts could be isolated from the reaction mixture, we cannot rule out the possible presence of this isomer.

In summary, condensation of either UPoC itself or the corresponding ester with aldehydes and ketones gives ready access to 1,3-dipoles either via formal 1,2-prototropic- or decarboxylative processes respectively.

The geometry within these 1,3-dipoles is predicted to be highly stereodefined and, due to their inherent asymmetry, they can undergo diastereoselective cycloadditions.

This stereocontrol is predicted to be particularly relevant in the case of the dipoles (**8**) derived from decarboxylation, where an intramolecular H-bond involving the N–H of the dipole and a carbonyl group of the uracil moiety restricts the conformational flexibility of the dipole relative to the sugar moiety and results in highly diastereoselective reactions via cycloaddition occurring from the most accessible face of the dipole. It should be possible to design a range of systems which take advantage of this ability to define the diastereofacial selectivity of such dipoles via remote H-bonding using appropriately-positioned substituents.

4.3. Bioactivity of compounds

The nikkomycin analogues (**6a-f**) were inactive at 125 μg/ml when tested against strains of *Aspergillus fumigatus*, and *Candida albians*.

5. Experimental

5.1. General

Nuclear magnetic resonance spectra were determined at 300, 400, 500 MHz Bruker spectrometers as specified. Chemical shifts are given in parts per million (δ) downfield from tetramethylsilane as internal standard. Spectra were determined in the solvent specified. The following abbreviations are used; s=singlet, d=doublet, t=triplet, q=quartet, m=multiplet, br=broad, brs=broad singlet and app=apparent.

Flash column chromatography was performed using silica gel 60 (230–400 mesh). Melting points were determined on a Kofler hot stage apparatus and are uncorrected. Microanalyses were obtained using a Carlo–Erba Model 1106 instrument. Mass spectra were recorded at 70 eV on a VG Autospec mass spectrometer. Specific rotations were measured at ambient temperature with an Optical Activity Ltd, AA-1000 polarimeter. All solvents were purified according to procedures given in Purification of Laboratory Chemicals, D. D. Perrin, W. L. F. Armarego, D. R. Perrin, Permagon Press, 1980.

5.1.1. Cycloadducts (6a) and (7a). A mixture of uracil polyoxin C (UpoC) (4) (0.1 g, 0.35 mmol), methyl pyruvate (0.071 g, 0.7 mmol) and NMM (0.04 g, 0.35 mmol) in degassed DMF (10 ml) was stirred and heated from room temperature to 70 °C over 30 min and heating at this temperature was maintained for 26 h under a N_2 atmosphere. Flash chromatography, eluting with 9:1 v/v EtOAc–ethanol afforded the product (0.144 g, 94%) as a 9:1 mixture of (**6a**) and (**7a**). Attempts to separate the isomers by crystallisation from CH_2Cl_2–petroleum ether (60–80 °C) resulted in the same 9:1 isomeric mixture as pale yellow prisms. The minor isomer could not be isolated in a pure form and was not studied further. Mp (mixed isomers) 147–152 °C, $[\alpha]_D^{20}$=+50.8 (C, 1 g/100 ml, EtOH). Found: C, 48.15; H, 4.6; N, 10.10. $C_{18}H_{22}N_4O_9.0.5H_2O$ requires: C, 48.3; H, 4.9; N, 12.5%. HRMS: 438.1465, $C_{18}H_{22}N_4O_9$ requires: 438.1474. *m/z* (%) (FAB): 439 (M+1, 49), 379 (5), 227 (29), 149 (9), 97 (31), 83 (43), 69 (61) and 55 (100).

5.1.2. Major isomer (6a): (1*R*,3*S*,3a*R*,6a*S*)-3-[(2′*R*,3′*S*,4′*R*,5′*R*)-5′-(2″,4″-dioxo-3″,5″-dihydro-2*H*-pyrimidin-1″-yl)-3″,4″-dihydroxy-tetrahydro-furan-2-yl]-1,5-dimethyl-4,6-dioxo-octahydro-pyrrolo[3,4-*c*]pyrrole-1-carboxylic acid methyl ester). δ (300 MHz) (acetone-d_6) assigned from the spectrum of the mixture: 9.96 (br, 1H, NHC=O), 8.32 (d, 1H, *J*=8.1 Hz, 6″-H), 5.84 (d, 1H, *J*=5.2 Hz, 5′-H), 5.5 (d, 1H, *J*=8.1 Hz, 5″-H), 4.2 (m, 3H, 2′-H, 3′-H, 4′-H), 4.0 (app. d, 1H, *J*=9.8 Hz, 3-H), 3.73 (s, 3H, CO_2Me), 3.51 (dd, 1H, *J*=8.1, 9.8 Hz, 3a-H), 3.32 (d, 1H, *J*=8.1 Hz, 6a-H), 2.6 (s, 3H, NMe) and 1.46 (s,

3H, Me). NOE data:

	Enhancement (%)								
Signal irradiated	6″-H	5′-*H*	5″-H	2′-H, 3′-H, 4′-H	3-H	3a-H	Me	6a-H	CO_2Me
6″-H		2.5	8.2	4.25					
5′-H				4.3					
5″-H	3.1								
2′-H, 3′-H, 4′-H	2.0	3.65			3.05				
3-H		1.3		11.3		7.95	6.0		
3a-H				4.3	5.65			4.4	
6a-H						1.75	2.75		2.0
CO_2Me							3.0		
Me					2.25			4.6	

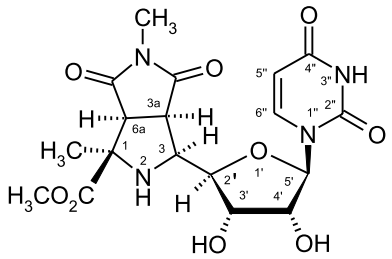

5.1.3. Cycloadducts (6b) and (7b). A stirred mixture of (UpoC) (4) (0.1 g, 0.35 mmol), methyl pyruvate (0.071 g, 0.7 mmol) and NPM (0.060 g, 0.35 mmol) in degassed DMF (10 ml) was heated from room temperature to 70 °C over 30 min and heating at this temperature was maintained for 26 h under a N_2 atmosphere. Flash chromatography, eluting with 10:1 v/v EtOAc–ethanol afforded the product (0.168 g, 96%) as a 12:1 mixture of (**6b**) and (**7b**) as a pale yellow amorphous solid. HPLC separation employed a Luna, C18 (2) 10 μm 250×4.6 mm, column eluting with 15:85 v/v MeCN/H_2O, flow rate: 0.7 ml/min with UV detection at 254 nm. The major isomer was obtained as pale yellow needles. Mp 161–164 °C, $[\alpha]_D^{20}$=+60.2 (C, 1 g/100 ml, EtOH). Found (mixed isomers): C, 53.6; H, 4.95; N, 10.2 $C_{23}H_{24}N_4O_9.H_2O$ requires: C, 53.3; H, 5.0; N, 10.8%. HRMS(ES): 523.1436, $C_{18}H_{23}N_4O_9Na$ requires: 523.1441. *m/z* (%) (FAB): 501 (M+1, 100), 441 (10), 329 (9), 287 (25) and 149 (10).

5.1.4. Major isomer (6b): (1*R*,3*S*,3a*R*,6a*S*)-3-[(2′*R*,3′*S*,4′*R*,5′*R*)-5′-(2″,4″-dioxo-3″,5″-dihydro-2*H*-pyrimidin-1″-yl)-3″,4″-dihydroxy-tetrahydro-furan-2-yl]-1-methyl-4,6-dioxo-5-phenyl-octahydro-pyrrolo[3,4-*c*]pyrrole-1-carboxylic acid methyl ester). δ (500 MHz) (acetone-d_6): 9.85 (br, 1H, NHC=O), 8.34 (d, 1H, *J*=8.1 Hz, 6″-H), 7.30 (m, 3H, Ar-H), 7.15 (m, 2H, Ar-H), 5.98 (d, 1H, *J*=5.8 Hz, 5′-H), 5.45 (d, 1H, *J*=8.1 Hz, 5″-H), 4.62 (br, 1H, NH), 4.45 (m, 1H, 2′-H), 4.41 (m, 1H, 4′-H), 4.38 (m, 1H, 3′-H), 4.10 (app. d, 1H, *J*=8.6 Hz, 3-H), 3.74 (s, 3H, CO_2Me), 3.68 (dd, 1H, *J*=8.6, 9.0 Hz, 3a-H), 3.59 (d, 1H, *J*=9.0 Hz, 6a-H), 2.76 (br, 2H, OH) and 1.54 (s, 3H, Me). ^{13}C(125 MHz) (acetone-d_6): 23.37 (CH), 46.34 (CH), 51.6 (CH), 55.89 (CH), 59.88 (CH), 67.28 (q), 72.33 (CH), 73.07 (CH), 81.83 (CH), 88.82 (CH), 102.49 (CH), 126.23 (2C, CH), 127.75 (CH), 128.34 (2C, CH), 132.95 (q), 141.86 (CH), 150.84 (q), 162.37 (q), 172.9 (q), 174.45 (q), 175.01 (q). *m/z* (%) (ES): 523 (M+Na, 100). NOE data:

	Enhancement (%)								
Signal irradiated	6″-H	5′-*H*	5″-H	4′-H	3-H	3a-H	3′-H	6a-H	CO_2Me
6″-H		4.65	13.8						
5″-H	7.67								
2′-H	1.0	3.0			6.2				
3-H				8.8		10.0	3.2		
6a-H						16.7			3.3
CO_2Me			1.0						
Me					2.65	1.0		3.9	1.0
4′-H	9.0				2.0				
3′-H	5.5				3.2				

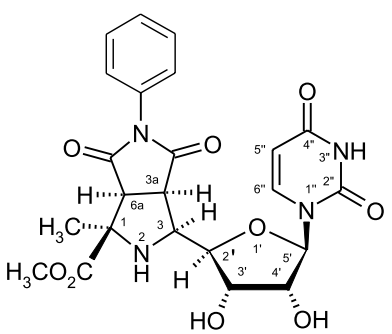

5.1.5. Cycloadducts (6c) and (7c). A stirred mixture of uracil polyoxin C(4) (0.1 g, 0.35 mmol), benzaldehyde (0.09 g, 0.76 mmol) and NMM (0.04 g, 0.35 mmol) in

degassed DMF (10 ml) was heated from room temperature to 80 °C over 30 min and heating at this temperature was maintained for 22 h under a N_2 atmosphere. Flash chromatography, eluting with 9:1 v/v EtOAc–ethanol afforded the product (0.121 g, 78%) as a 3:1 mixture of (**6c**) and (**7c**). The isomeric mixture crystallised from CH_2Cl_2–petroleum ether (60–80 °C) as pale yellow prisms. Mp 173–177 °C. Found: C, 55.25; H, 4.95; N, 12.5, $C_{21}H_{22}N_4O_7.0.5H_2O$ requires: C, 55.85; H, 5.15; N, 12.4%. HRMS: 442.1488. $C_{21}H_{22}N_4O_7$ requires: 442.1495 *m/z* (%) (FAB): 443 (M+1, 100), 331 (19), 229 (55), 144 (18) and 69 (22).

5.1.6. Major isomer (6c): (1*R*,3*S*,3a*R*,6a*S*)-3-[(2′*R*,3′*S*,4′*R*,5′*R*)-5′-(2′,4′-dioxo-3′,5′-dihydro-2*H*-pyrimidin-1″-yl)-3″,4″-dihydroxy-tetrahydro-furan-2-yl]-5-methyl-1-phenyl-tetrahydro-pyrrolo[3,4-*c*]pyrrole-4,6-dione). δ (400 MHz) (acetone-d_6) assigned from the spectrum of the isomeric mixture: 10.2 (br, 1H, NHC═O), 7.8 (d, 1H, *J*=8.1 Hz, 6″-H), 7.3–7.2 (m, 5H, Ar-H), 5.90 (d, 1H, *J*=4.5 Hz, 5′-H), 5.61 (d, 1H, *J*=8.1 Hz, 5″-H), 4.8 (d, 1H, *J*=8.4 Hz, 1-H), 4.0 (m, 1H, 4′-H), 4.33 (m, 1H, 3′-H), 4.41 (m, 1H, 2′-H), 3.90 (app. d, 1H, *J*=7.5 Hz, 3-H), 3.56–3.49 (m, 2H, 3a-H and 6a-H) and 2.74 (s, 3H, NMe). NOE data:

Signal irradiated	Enhancement (%)									
	6″-H	5′-*H*	5″-H	1-H	4′-H	3′-H	2′-H	3-H	3a-H, 6a-H	Ar-H
6″-H		5.5	7.5							
5′-*H*	3.5				2.5		2.7			
5″-					7.2					
1-H							9.7	4.9	11.8	12.6
4′-H	5.2									
3′-H	3.45	5.7				4.1		7.7	4.35	
2′-H		4.5		5.65					4.7	
3-H						8.2			4.2	
3a-H, 6a-H				6.2	4.2		5.5	4.2		

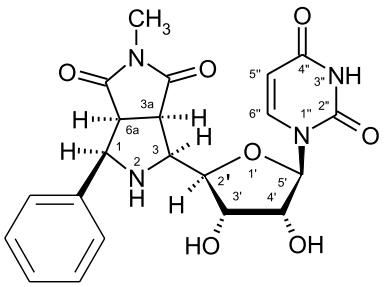

5.1.7. Minor isomer(7c): (1*S*,3*R*,3a*S*,6a*R*)-3-[(2′*R*,3′*S*,4′*R*,5′*R*)-5′-(2′,4′-dioxo-3′,5′-dihydro-2*H*-pyrimidin-1″-yl)-3″,4″-dihydroxy-tetrahydro-furan-2-yl]-5-methyl-1-phenyl-tetrahydro-pyrrolo[3,4-*c*]pyrrole-4,6-dione. δ (400 MHz) (acetone-d_6) assigned from the spectrum of the isomeric mixture: 10.2 (br, 1H, NHC═O), 7.8 (d, 1H, *J*=8.1 Hz, 6″-H), 7.3–7.2 (m, 5H, Ar-H), 5.90 (d, 1H, *J*=4.5 Hz, 5′-H), 5.72 (d, 1H, *J*=8.1 Hz, 5″-H), 4.9 (d, 1H, *J*=8.4 Hz, 1-H), 4.65 (m, 1H, 4′-H), 4.40 (m, 1H, 3′-H), 4.41 (m, 1H, 2′-H), 3.90 (app. d, 1H, *J*=7.5 Hz, 3-H), 3.56–3.49 (m, 2H, 3a-H and 6a-H) and 2.73 (s, 3H, NMe).

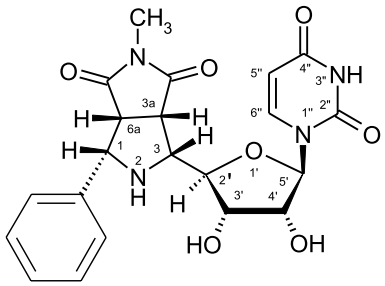

5.1.8. Cycloadducts (6d) and (7d): (1*R*,3*S*,3a*R*,6a*S*)-3-[(2′*R*,3′*S*,4′*R*,5′*R*)-5′-(2″,4″-dioxo-3′,5′-dihydro-2*H*-pyrimidin-1″-yl)-3″,4″-dihydroxy-tetrahydro-furan-2-yl]-5-methyl-1-pyridin-2yl-tetrahydro-pyrrolo[3,4-*c*]pyrrole-4,6-dione) and (1*S*,3*R*,3a*S*,6a*R*)-3-[(2′*R*,3′*S*,4′*R*,5′*R*)-5′-(2″,4″-dioxo-3′,5′-dihydro-2*H*-pyrimidin-1″-yl)-3″,4″-dihydroxy-tetrahydro-furan-2-yl]-5-methyl-1-pyridin-2yl-tetrahydro-pyrrolo[3,4-*c*]pyrrole-4,6-dione). A stirred mixture of uracil polyoxin C(4) (0.1 g, 0.35 mmol), pyridine-2-carboxaldehyde (0.15 g, 1.4 mmol) and NMM (0.04 g, 0.35 mmol) in degassed DMF (10 ml) was heated from room temperature to 65 °C over 30 min and heating at this temperature was maintained for 24 h under a N_2 atmosphere. Flash chromatography, eluting with 9:1 v/v EtOAc–ethanol afforded the product (0.08 g, 55%) as a 4:3 mixture of isomers together with trace amounts of a third isomer. The mixed isomers crystallised from CH_2Cl_2–petroleum ether (60–80 °C) as pale yellow prisms. Mp 169–174 °C. HRMS: 443.1446, $C_{20}H_{21}N_5O_7$ requires: 443.1441, δ (400 MHz) (MeOH-d_4) (mixed isomers): 8.44 (d, 1H, *J*=4.8 Hz, pyridine-H, isomers), 7.83 (d, 1H, *J*=8.1 Hz, 6″-H, isomers), 7.72 (m, 1H, pyridine-H, isomers), 7.82 and 7.25 (2×m, 2H, pyridine H), 5.85 and 5.82 (2×d, 1H, *J*=4.7 Hz, 6a-H and 5′-H isomers), 5.77 and 5.65 (2×d, 1H, *J*=8.1 Hz, 5″-H, isomers), 4.28 (m, 2H, 1-H, and 4′-H, isomers), 4.01 (m, 2H, 6a-H and 3′-H, isomers), 3.61 and 3.46 (2×m, 3H, 3a-H, 2′-H and 3′-H isomers) and 2.75 (25, 3H, *N*Me, isomers). *m/z* (%) (FAB): 444 (M+1, 94), 332 (12), 230 (32), 113 (45), 97 (23), 83 (46), 69 (77) and 57 (100).

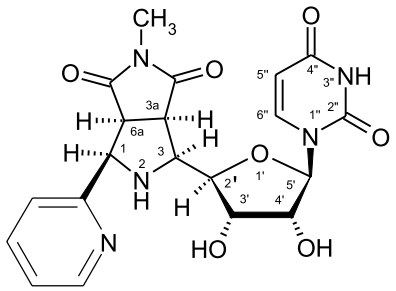

(6d)

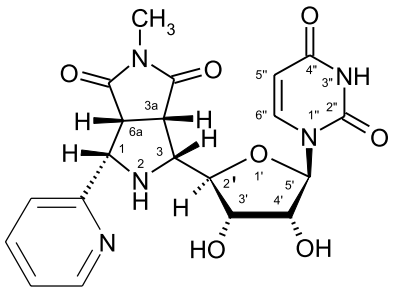

(7d)

5.1.9. Cycloadducts (6e) and (7e): (1*R*,3*S*,3a*R*,6a*S*)-1-(1-benzenesulphonyl-1-*H*-indol-3-yl)-3-[(2′*R*,3′*S*,4′*R*,5′*R*)-5′-(2″,4″-dioxo-3″,4″-dihydro-2*H*-pyrimidin-1-yl)-3″,4″-dihydroxy-tetrahidro-furan-2-yl]-5-methyl-tetrahydro-pyrrolo[3,4-*c*]pyrrole-4,6-dione) (6e) and (1*S*,3*R*,3a*S*,6a*R*)-1-(1-benzenesulphonyl-1-*H*-indol-3-yl)-3-[(2′*R*,3′*S*,4′*R*,5′*R*)-5′-(2″,4″-dioxo-3″,4″-dihydro-2*H*-pyrimidin-1-yl)-3″,4″-dihydroxy-tetrahydro-furan-2-yl]-5-methyl-tetrahydro-pyrrolo[3,4-*c*]pyrrole-4,6-dione) (7e). A stirred mixture of uracil polyoxin C (0.1 g, 0.35 mmol), *N*-sulphonyl indole-3-carboxaldehyde (0.19 g, 0.7 mmol) and NMM (0.04 g, 0.35 mmol) in degassed DMF (10 ml) was heated from room temparature to 80 °C over 30 min and heating at this temperature was maintained for 24 h under N_2. Flash chromatography, eluting with 9:1 v/v EtOAc–ethanol afforded the product (0.16 g, 72%) as a 1:1 mixture of isomers. Crystallisation from CH_2Cl_2–petroleum ether (60–80 °C) gave one isomer, slightly contaminated with the other isomer, as pale yellow amorphous solid. Mp 167–171 °C. $[\alpha]_D^{20}$=+12 (0.5 g/100 ml EtOH. Found (mixed isomers): C, 54.75; H, 4.7; N, 10.7; S, 4.95; $C_{29}H_{27}N_5O_9$ S.H_2O: C, 54.45; H, 4.5; N, 10.90, S, 5.0%. *m/z* (%) (FAB): 622 (M+1, 100), 510 (19), 480 (22), 408 (28) and 365 (14), 113 (19), 97 (31), 83 (45) and 69 (74).

Compound (**6e**). Found: C, 55.35; H, 4.55; N, 10.75: S, 5.1, $C_{29}H_{27}N_5O_9$ S.0.5H_2O requires: C, 55.25; H, 4.45; N, 11.1, S, 5.1%. HRMS: 621.1517 $C_{29}H_{27}N_5O_9$ S.H_2O requires: 621.1529. δ (400 MHz) (Methanol-d_6): 10.2 (br, 1H, NHC=O), 8.4–7.6 (m, 11H, Ar-H, 6″-H and CH=C), 5.80 (d, 1H, 4.5 Hz, 5′-H), 5.32 (d, 1H, *J*=8.1 Hz, 5″-H), 4.9 (br, 1H, 2′-H), 4.40–4.35 (m, 2H, 4′-H+2-H), 4.30 (app. t, 1H, *J*=4.6 Hz, 1-H), 3.94 (dd, 1H, *J*=8.9, 4.6 Hz, 6a-H), 3.90 (app. d, 1H, *J*=7.0 Hz, 3-H), 3.75 (d, 1H, *J*=7.8 Hz, 3′-H), 3.66 (dd, 1H, *J*=8.9, 7.0 Hz, 3a-H) and 2.85 (s, 3H, *N*Me). *m/z* (%) (FAB): 622 (M+H, 100), 510 (21), 408 (42), 127 (44), 113 (35) and 69 (23).

5.1.10. Cycloadducts (6f) and (7f). A mixture of uracil polyoxin C(4) (0.1 g, 0.35 mmol), isatin (0.12 g, 0.70 mmol) and NMM (0.04 g, 0.35 mmol) in degassed DMF (10 ml) was heated from room temperature to 90 °C over 30 min and heating at this temperature was maintained for 30 h under a N_2 atmosphere. Flash chromatography, eluting with 9:1 v/v EtOAc–ethanol afforded the product (0.138 g, 82%) as a 2:1 isomer mixture. Crystallisation from CH_2Cl_2–petroleum ether (60–80 °C) resulted in the same 2:1 isomeric mixture as a pale yellow amorphous solid. Mp 254–259 °C. Found (mixed isomers): C, 50.6; H, 4.5; N, 13.8. $C_{22}H_{22}N_5O_8$ 2.H_2O requires: C, 50.85; H, 4.8; N, 13.5%. *m/z* (%) (FAB): 484 (M+1, 100), 312 (20), 270 (51), 185 (20), 113 (20) and 77 (10).

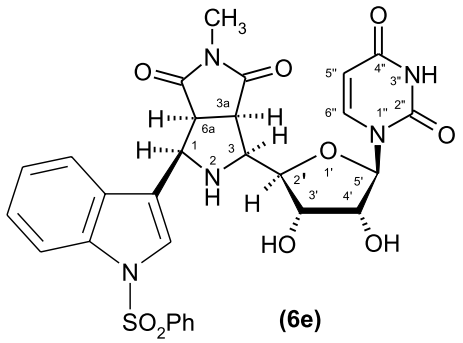

(6e)

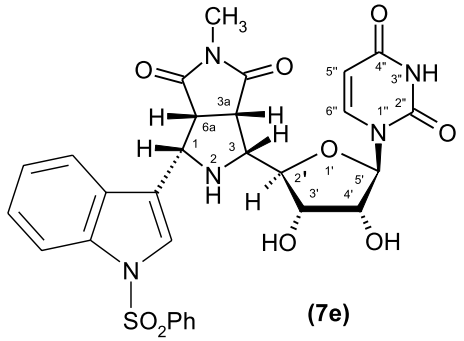

(7e)

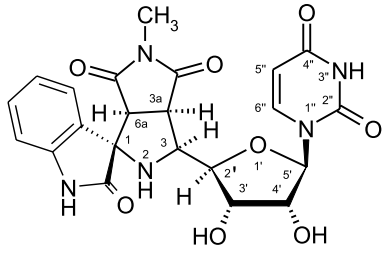

(6f)

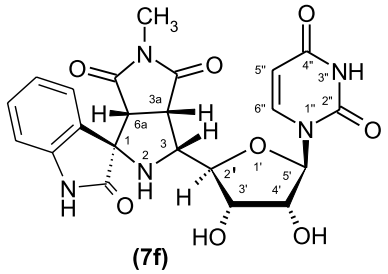

(7f)

5.1.11. Major isomer (6f). δ (400 MHz) (MeOH-d_4) assigned from the spectrum of the isomeric mixture: 8.0 (d, 1H, *J*=8.1 Hz, 6”-H), 7.3–6.8 (m, 4H, Ar-H), 5.80 (d,

1H, J=4.8 Hz, 5′-H), 5.64 (d, 1H, J=8.1 Hz, 5″-H), 4.61 (d, 1H, J=8.2 Hz, 6a-H), 4.42 (m, 1H, 2′-H), 4.15 (m, 2H, 3′-H+4′-H), 3.72 (app. t, 1H, J=8.2 Hz, 3a-H), 3.43 (app. d, 1H, J=8.2 Hz, 3-H) and 2.91 (s, 3H, *N*Me).

5.1.12. Minor isomer (7f). δ (400 MHz) (MeOH-d_4) assigned from the spectrum of the isomeric mixture: 7.68 (d, 1H, J=8.1 Hz, 6″-H), 7.3–6.8 (m, 4H, Ar-H), 5.82 (d, 1H, J=4.8 Hz, 5′-H), 5.73 (d, 1H, J=8.1 Hz, 5″-H), 4.63 (d, 1H, J=8.6 Hz, 6a-H), 4.24 (m, 1H, 2′-H), 4.15 (m, 2H, 3′-H+4′-H), 4.52 (dd, 1H, J=8.6, 7.8 Hz, 3a-H), 3.50 (app. d, 1H, J=7.8 Hz, 3-H) and 3.0 (s, 3H, *N*Me).

5.1.13. (1*S*,3*S*,3a*S*,6a*R*)-3-[(2′*R*,3′*S*,4′*R*,5′*R*)-5′-(2″,4″-Dioxo-3″,4″-dihydro-2*H*-pyrimidin-1-yl)-3″,4″-dihydroxy-tetrahydro-furan-2-yl]-5-methyl-4,6-dioxo-1-phenyl-octahydro-pyrrolo[3,4-*c*]pyrrole-1-carboxylic acid methyl ester) (11). UPoC methyl ester hydrochloride (**9**)[13] (0.15 g, 0.45 mmol), NMM (0.055 g, 0.5 mmol), benzaldehyde (0.1 g, 0.9 mmol) and anhydrous magnesium sulphate (0.5 g) were stirred in pyridine (15 ml) at 100 °C for 28 h. Dichloromethane was added to the cooled solution which was then washed with water (2×20 ml), dried ($MgSO_4$), filtered and the filtrate evaporated under reduced pressure. Flash chromatography of the residue, eluting with 9:1 v/v EtOAc–EtOH afforded (11) (0.07 g, 32%) as a brown solid. Attempted crystallisation from CH_2Cl_2–petroleum ether (60–80 °C) afforded a pale brown amorphous solid. Mp 154–159 °C. HRMS: 500.1569, $C_{23}H_{24}N_4O_9$ requires: 500.1569, δ (400 MHz), (acetone-d_6): 10.1 (br, 1H, NHC=O), 7.66 (d, 1H, J=8.1 Hz, 6″-H), 7.4–7.1 (m, 5H, Ar-H), 5.65 (m, 2H, 5′-H, 5″-H), 5.16 (t, 1H, J=6.1 Hz, 2′-H), 5.0 (1H, d, J=6.8 Hz, *N*H), 4.94 (dd, 1H, J=8.2, 6.8 Hz, 1-H), 3.78 (dd, 1H, J=8.2, 5.1 Hz, 6a-H), 3.45 (d, 1H, J=5.1 Hz, 3a-H), 3.43 (s, 3H, OMe) and 2.80 (s, 3H, *N*Me). *m*/*z* (%) (FAB): 501 (M+1, 10), 149 (20), 109 (18), 95 (34), 81 (48), 69 (72) and 55 (100). NOE data:

	Enhancement (%)										
Signal irradiated	6″-H	5′-*H*, 5″-H	2′-H	1-H	3′-H	4′-H	6a-H	3a-H	Ar-H	OMe	NH
6″-H		11.4									
5′-*H*, 5″-H	7.6				1.6	2.5				4.5	
2′-H					2.0	5.2		2.9			
1-H							10.6		11.2		
3′-H		5.0	4.9								
4′-H	4.3	10.1			7.9					1.4	9.2
6a-H				10.2				8.45			
3a-H			5.1				12.3				
CO_2Me	3.9	8.1			4.9				10.25		

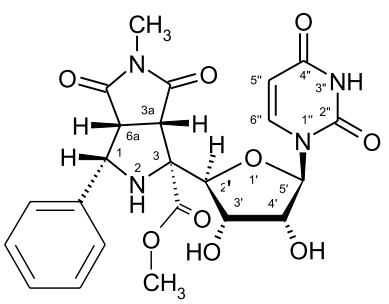

11

5.2. Single-crystal X-ray analysis

Crystallographic data for **6b** was measured on a Nonius Kappa CCD area-detector diffractometer using a mixture of area detector ω- and ϕ-scans and graphite monochromated Mo K_α radiation (λ=0.71073 Å). The structure was solved by direct methods using SHELXS-86[17] and were refined by full-matrix least-squares (based on F^2) using SHELXL-97.[18] The weighting scheme used was $w=[\sigma^2(F_o^2)+(0.1148P)^2+3.8871P]^{-1}$ where $P=(F_o^2+2F_c^2)/3$. All non-hydrogen atoms were refined with anisotropic displacement parameters whilst hydrogen atoms were constrained to predicted positions using a riding model. The final absolute configuration was based on the known chirality of the uracil polyoxin starting material. The residuals wR_2 and R_1, given below, are defined as $wR_2=(\sum[w(F_o^2-F_c^2)^2]/\sum[wF_o^2]^2)^{1/2}$ and $R_1=\sum||F_o|-|F_c||/\sum|F_o|$.

Full supplementary crystallographic data, which include hydrogen co-ordinates, thermal parameters and complete bond lengths and angles, have been deposited at the Cambridge Crystallographic Data Centre and are available on request.(**6b**, CCDC 214092).

Crystal data for **6b**. $C_{23}H_{24}N_4O_9.H_2O$, 0.31×0.31×0.13 mm, M=518.48, trigonal, space group $R\bar{3}$, a=25.5247(9), c=9.9448(3) Å, U=5611.1(3) Å^3, Z=4, D_c=1.38 Mg m^{-3}, μ=0.11 mm^{-1}, F(000)=2448, T=150 K.

Data collection. 1.0<2θ<52.0°; 4863 unique data were collected [R_{int}=0.052]; 4248 reflections with F_o >4.0 $\sigma(F_o)$.

Structure refinement. Number of parameters=339, goodness of fit, s=1.043; wR_2=0.1698, R_1=0.0607.

Acknowledgements

We thank the University of Leeds, Mersin University, the Royal Society and TUBITAK-Turkey for support and Dr. A. K. Saksena (Schering-Plough), for a generous gift of uracil polyoxin C.

References and notes

1. (a) Zahner, H.; Holst, H.; Zeobelein, G.; Keckeisen, A. US

Patent 4287186, 1981. (b) Dahn, U.; Hagenmaier, H.; Hohne, H.; Konig, W. A.; Wolf, G.; Zaher, H. *Arch. Microbiol.* **1976**, *107*, 143–160.
2. (a) Uramoto, M.; Kobinata, K.; Isono, K.; Higashisima, T.; Miyazawa, T.; Jenhins, E. E.; McCloskey, J. A. *Tetrahedron Lett.* **1980**, *21*, 3395–3398. (b) Uramoto, M.; Kobinata, K.; Isono, K.; Higashisima, T.; Miyazawa, T.; Jenhins, E. E.; McCloskey, J. A. *Tetrahedron* **1982**, *38*, 1599–1608. (c) Kobinata, K.; Uramoto, M.; Nishii, M.; Isono, K. *Agric. Biol. Chem.* **1980**, *44*, 1709–1711. (d) Obi, K.; Uda, J.; Iwase, K.; Sugimoto, O.; Ebusu, H.; Matsuda, A. *Bioorg. Med. Chem. Lett.* **2000**, *10*, 1451–1454. (e) Uda, J.; Obi, K.; Iwase, K.; Sugimoto, O.; Ebusu, H.; Matsuda, A. *Nucleic acids Symposium Series (26th Symposium on Nucleic acids Chemistry)*, **1999**, *13–14*. (f) Kiyoto, T.; Yatsuji, A.; Kajita, T.; Miyao, N.; Nomura, N. Jpn. Kokai Tokkyo Koho, 1999, 45pp. (g) Cooper, A. B.; Saksena, A. K.; Lovey, R. G.; Grija-vallabhan, V. M.; Ganguly, A. US, 1994, 25pp. (h) Krainer, E.; Becker, J. M.; Naider, F. *J. Med. Chem.* **1991**, *34*, 174–180.
3. Isono, K. *J. Antibiot.* **1988**, *41*, 1711–1739, and references cited therein.
4. (a) Auberson, Y.; Vogel, P. *Tetrahedron* **1990**, *46*, 7019–7032. (b) Barrett, A. G. M.; Lebold, S. A. *J. Org. Chem.* **1991**, *56*, 4875–4884. (c) Barluenga, J.; Viado, A. L.; Aguilar, E.; Fustero, S.; Olano, B. *J. Org. Chem.* **1993**, *58*, 5972–5975. (d) Garner, P.; Park, J. M. *Tetrahedron Lett.* **1989**, *30*, 5065–5068. (e) Cooper, A. B.; Desai, J.; Lovey, R. G.; Saksena, A. K.; Grija-Vallabhan, V. M.; Gangulonely, A. K.; Loebenberg, D.; Parmegiani, R.; Cacciapuoti, A. *Bioorg. Med. Chem. Lett.* **1993**, *3*, 1079–1084.
5. Isono, K.; Asahi, K.; Suzuki, S. *J. Am. Chem. Soc.* **1969**, *91*, 7490–7505.
6. (a) Isono, K.; Nagatsu, J.; Kawashima, Y.; Suzuki, S. *Agric. Biol. Chem.* **1965**, *29*, 848–854. (b) Isono, K.; Nagatsu, J.; Kobinata, K.; Sasaki, K.; Suzuki, S. *Agric. Biol. Chem.* **1967**, *31*, 190–199.
7. Shenbagamurthi, P.; Smith, H. A.; Becker, J. M.; Steinfeld, A.; Naider, F. *J. Med. Chem.* **1983**, *26*, 1518–1522.
8. Grigg, R.; Surendrakumar, S.; Thianpatanagul, S.; Vipond, D. *J. Chem. Soc., Perkin Trans. 1* **1988**, 2693–2701.
9. (a) Aly, M. F.; Grigg, R.; Thianpatanagul, S.; Sridharan, V. *Chem. Soc., Perkin Trans. 1* **1988**, 949–955. (b) Grigg, R.; Henderson, D.; Hudson, A. J. *Tetrahedron Lett.* **1989**, *30*, 2841–2844.
10. Grigg, R.; Aly, M. F.; Sridharan, V.; Thianpatanagul, S. *J. Chem. Soc., Chem. Commun.* **1984**, 182–183.
11. Grigg, R.; Idle, J.; McMeekin, P.; Surendrakumar, S.; Vipond, D. *J. Chem. Soc., Perkin Trans. 1* **1988**, 2703–2713.
12. Ardill, H.; Grigg, R.; Malone, J. F.; Sridharan, V.; Thomas, W. A. *Tetrahedron* **1994**, *50*, 5067–5082.
13. Cooper, D. M. Thesis submitted to the School of Chemistry, Leeds University: Leeds, 1996.
14. Azuma, T.; Isono, K. *J. Chem. Soc., Chem. Commun.* **1977**, 159–160.
15. Calculations were performed using the AM1 Hamiltonian and the COSMO force field to simulate the appropriate reaction solvent field as described by Klant, A.; Schuurman, G. *J. Chem. Soc., Perkin Trans. 2* **1993**, 799.
16. Desiraju, G. R.; Steiner, T. *The weak hydrogen bond*; Oxford University Press: Oxford, 1999.
17. Sheldrick, G. M. *Acta Crystallogr.* **1990**, *A46*, 467–473.
18. Sheldrick, G. M. *SHELX-93. Program for Refinement of Crystal Structures*; Universty of Gottingen: Germany, 1993.